



CrossMark

Journal of Taibah University for Science 11 (2017) 76–84

Journal
of Sciencewww.elsevier.com/locate/jtusci

Synthesis, growth, and structural, optical, mechanical, electrical properties of a new inorganic nonlinear optical crystal: Sodium manganese tetrachloride (SMTC)

M. Packiya raj^a, S.M. Ravi Kumar^{b,*}, R. Srineevasan^b, R. Ravisankar^b

^a Department of Physics, S.K.P. Engineering College, Tiruvannamalai 606611, Tamilnadu, India

^b PG & Research Department of Physics, Government Arts College, Tiruvannamalai 606603, Tamilnadu, India

Received 3 July 2015; received in revised form 8 August 2015; accepted 9 August 2015

Available online 10 November 2015

Abstract

A new inorganic nonlinear optical single crystal of sodium manganese tetrachloride (SMTC) has been successfully grown from aqueous solution using the slow evaporation technique at room temperature. The crystals obtained using the aforementioned method were characterized using different techniques. The crystalline nature of the as-grown crystal of SMTC was analyzed using powder X-ray diffraction. Single-crystal X-ray diffraction revealed that the crystal belongs to an orthorhombic system with non-centrosymmetric space group Pbam. The optical transmission study of the SMTC crystal revealed high transmittance in the entire UV–vis region, and the lower cut-off wavelength was determined to be 240 nm. The mechanical strength of the as-grown crystal was estimated using the Vickers microhardness test. The second harmonic generation (SHG) efficiency of the crystal was measured using Kurtz's powder technique, which indicated that the crystal has a nonlinear optical (NLO) efficiency that is 1.32 times greater than that of KDP. The dielectric constant and dielectric loss of the compound were measured at different temperatures with varying frequencies. The photoconductivity study confirmed that the title compound possesses a negative photoconducting nature. The growth mechanism and surface features of the as-grown crystals were investigated using chemical etching analysis.

© 2015 The Authors. Production and hosting by Elsevier B.V. on behalf of Taibah University. This is an open access article under the CC BY-NC-ND license (<http://creativecommons.org/licenses/by-nc-nd/4.0/>).

Keywords: Sodium manganese tetrachloride; XRD; Second harmonic generation

1. Introduction

The well-known properties of laser radiation are important for a wide range of applications. Laser

radiation can be converted from one form of frequency to another through nonlinear optics; hence, the application of nonlinear optics has significantly increased in various fields of science and technology. In general, a nonlinear optical (NLO) interaction is produced by one or two laser beams incident on a suitable material in which an output beam with the desired frequency is produced [1,2]. Harmonic generation, sum and difference frequency generation and parametric oscillation are included in the NLO interaction [3]. A lower frequency pair of tuneable output beams can be produced only by a suitable material when it interacts (NLO) with a high

* Corresponding author. Tel.: +91 8608953139.

E-mail address: smravi78@rediffmail.com (S.M. Ravi Kumar).

Peer review under responsibility of Taibah University.

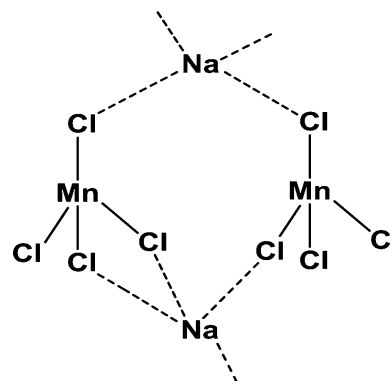


input laser beam. The NLO interaction imposes several demands on potential NLO materials. The field of nonlinear optics is currently one of the most attractive fields of research because of its vital applications in various areas, such as optical switching, optical data storage for developing technologies in telecommunications and signal processing [4–6]. The first demonstration of NLO was performed in 1961, which revealed that nonlinear frequency conversion is a field with highly limited materials [7]. Therefore, materials should be optically transparent, possess a quadratic susceptibility of sufficient magnitude, allow for phase-matching interaction and withstand the laser intensity without damage. To date, the most important class of materials used in nonlinear optics is inorganic single crystals.

Inorganic materials that exhibit second-order nonlinear optical properties have attracted interest in the recent past due to their ability to be processed into crystals, wide optical transparency domain, large nonlinear figure of merit for frequency conversion, fast optical response time and wide phase-matchable angle [8]. These ionic-bonded inorganic crystals are easy to synthesize, and they have a high melting point and high degree of chemical inertness [9]. In 1961, Franken et al. observed highly polarizable inorganic crystals and their efficient active second-order harmonic generation (SHG) [7].

Inorganic materials have advantages over organic materials, such as architectural flexibility for molecular design and morphology, high mechanical strength and good environmental stability with non-toxicity and usability in high-power applications. The molecular hyperpolarizability of inorganic nonlinear optical crystals is used in optical switching (modulation), frequency conversion (SHG, wave mixing) and electro-optic applications, particularly in EO modulation. Historically, inorganic NLO materials have been chronicled more extensively than inorganic oxide crystals. LiNbO₃, KNbO₃, KDP and KTP, among others, have been studied for device applications, such as piezoelectric, ferroelectric and electro-optic applications [10]. These materials have also been successfully used in commercial frequency doublers, mixers and parametric generators to provide coherent laser radiation with high frequency conversion efficiency in the new region of the spectrum, which is inaccessible by other conventional nonlinear crystal sources.

The aim of this research work is to investigate the processing and properties of the inorganic nonlinear optical crystal sodium manganese tetrachloride (SMTC) with molecular formula Na₂MnCl₄ used in NLO frequency conversion. The structure of Na₂MnCl₄ was determined by Goodyear et al. in 1971 [11]. In the



Scheme 1. Molecular arrangement of SMTC crystal.

SMTC crystals, chlorine ions are octahedrally coordinated with Mn ions, form an infinite chain parallel to the *c* axis and are held with sodium ions. The sodium ions are surrounded by four chloride ions, which are located at the corners of a trigonal prism. The binding of Mn–Cl and Na–Cl suggests that the structure is primarily ionic in character. Hence, an attempt has been made to grow sodium manganese tetrachloride (SMTC) single crystals using the slow evaporation solution growth technique, and its physical and chemical properties have been investigated for the first time.

2. Experimental procedure

2.1. Synthesis

SMTC salt was synthesized by combining analytical reagent (AR)-grade manganese chloride and sodium chloride in a stoichiometric ratio of 1:2 with double-distilled water as a solvent. The synthesized SMTC salt was obtained based on the following chemical reaction:



Manganesechloride + sodiumchloride
→ sodiummanganesetetrachloride.

The scheme for the molecular structure of SMTC is shown in [Scheme 1](#).

2.2. Solubility study

The growth rate of a crystal depends on its solubility and temperature. Solvent and solubility factors define super saturation, which is the driving force for the rate of crystal growth. The solubility study was performed

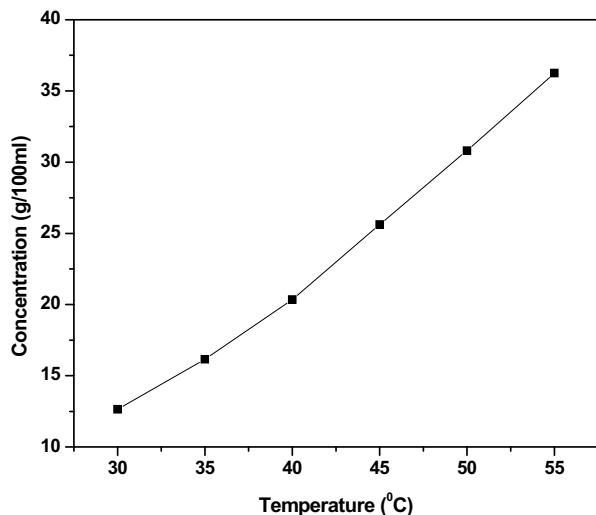


Fig. 1. Solubility curve of SMTC.

by adding an excess of SMTC to the solvent, and it was continuously stirred to achieve a uniform concentration throughout the entire volume of the solution. The solubility of SMTC in the solvent of double-distilled water was determined for various temperatures between 30 °C and 55 °C in 5 °C intervals using a constant temperature bath with an accuracy of ± 0.01 °C attached to a cryostat. After reaching saturation, the solute concentration was analyzed gravimetrically. The solubility curve for SMTC is shown in Fig. 1. As shown in this figure, SMTC has a positive solubility (i.e., the solubility increases linearly with temperature) gradient in water.

2.3. Crystal growth

The prepared solutions were vigorously stirred at RT for 4 h. Continuous stirring with slight increases in temperature ensures homogeneity and avoids the co-precipitation of motifs. Purification of the synthesized salt was achieved by successive recrystallization processes. The saturated mixture was filtered two times with micron pore size Whatman filter paper. This synthesized clean solution was poured into a Petri dish and covered with polythene paper with pores, which allowed for slow evaporation of the water solvent. After a duration of 35 days, the solvent had evaporated and good quality SMTC crystals with dimensions of 2 mm \times 2 mm \times 1 mm were harvested from the Petri dish. The growth rate was determined to be 0.12 mm per day. The as-grown crystal was defect free, optically transparent and contained no inclusions. The as-grown crystal of SMTC is shown in Fig. 2.

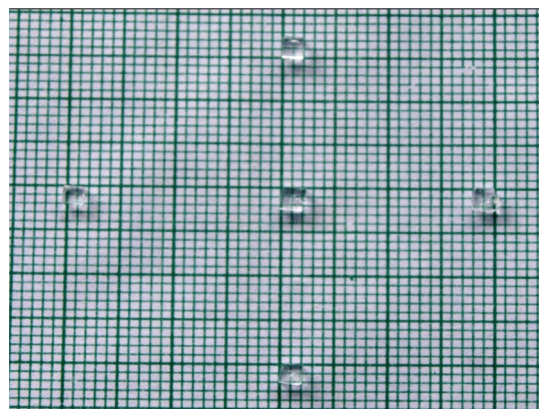


Fig. 2. Photograph of as-grown crystals of SMTC.

3. Characterization of SMTC single crystal

The as-grown crystal of SMTC was subjected to single-crystal and powder XRD analyses using an Enraf-Nonius CAD4 X-ray diffractometer and a Bruker D8 Advance (Germany) X-ray diffractometer, respectively. The transmission behaviour of the as-grown crystal was studied using a LAMBDA 35 UV–vis spectrophotometer. The NLO efficiency of the as-grown crystal was tested using the Kurtz powder technique with a ND:YAG laser with a wavelength of 1064 nm. The mechanical behaviour of the as-grown sample was investigated using a Vickers microhardness tester. Dielectric constant and dielectric loss studies were performed using a Hioki 3532 LCR HiTESTER. A Keithley 485 picoammeter was used to investigate the photoconductivity of the as-grown SMTC crystal.

3.1. Results and discussion

3.1.1. Single-crystal XRD studies

The single-crystal XRD study indicated that the unit cell parameters of the as-grown SMTC crystals are $a = 6.93$ Å, $b = 11.82$ Å, $c = 3.86$ Å, and $\alpha = \beta = \gamma = 90^\circ$, and thus, the volume of the cell is 316.182 Å³. Hence, the SMTC crystal is an orthorhombic structure with space group Pbam. The lattice parameters are in good agreement with the reported values [11].

3.1.2. Powder XRD studies

Powder XRD of as-grown SMTC crystals was conducted, and the XRD pattern is shown in Fig. 3. The powder sample was scanned over the range of 10–80° at a scan rate of 0.2°/s using CuK α radiation with a wavelength of 1.545 Å. The obtained powder X-ray diffraction data were analyzed and compared with

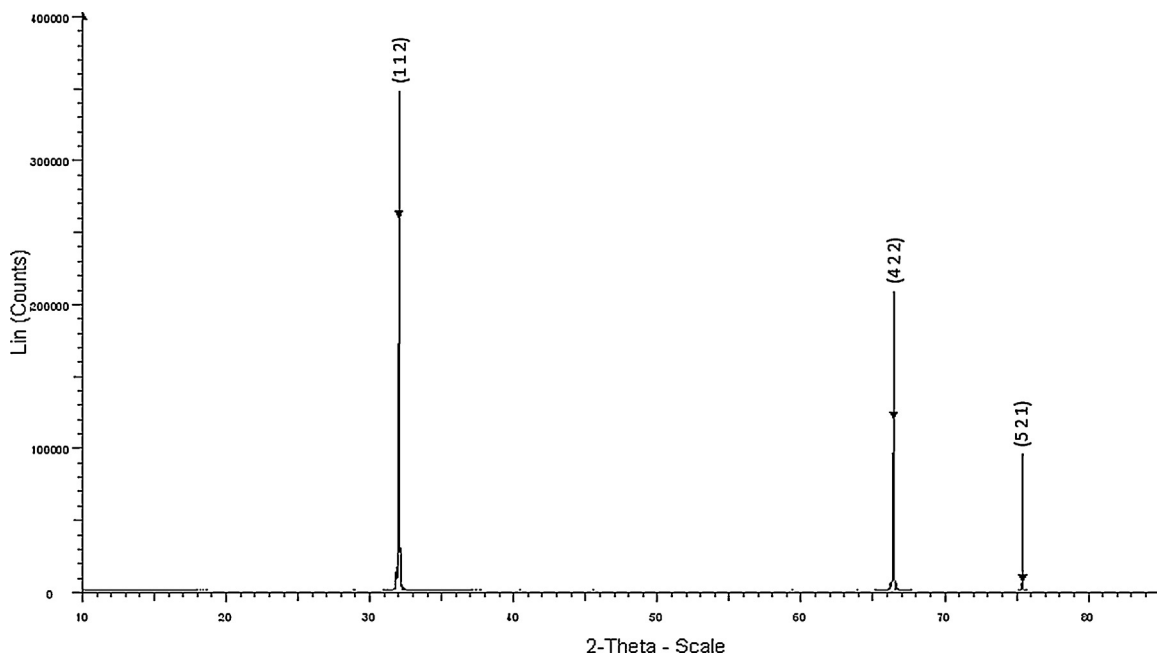


Fig. 3. Powder XRD pattern of SMTC.

JCPDS data (JCPDS card number 4137). The limited number of sharp peaks without any broadening in the XRD pattern confirms that the as-grown SMTC possesses good crystallinity.

3.1.3. Linear optical transmission studies

Because NLO crystals are only of practical use when they possess a wide transparency window, the transmission range of the SMTC crystal was determined by recording the optical transmission spectrum in the wavelength region of 200–900 nm. The optical transmission spectrum of the SMTC crystal is shown in Fig. 4. An optically polished single crystal with a thickness of 2 mm was

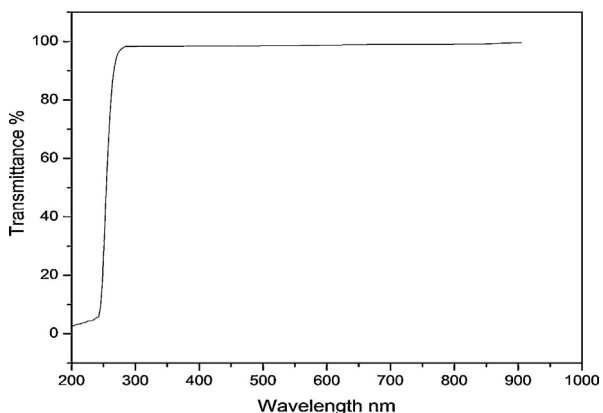


Fig. 4. UV–vis spectrum of SMTC crystal.

used to study the transmission behaviour of SMTC. This recorded spectrum provides information about the structure of the molecule based on the absorption of UV and visible light, which involves the promotion of electrons in the σ and π orbitals from the ground state to a higher energy state [12]. The transmission spectrum shows that the as-grown crystal has a lower cut-off wavelength at 240 nm, which is attributed to electronic transmission in the SMTC crystal. Absence of absorbance in the region between 240 nm and 900 nm is an essential property for nonlinear optical crystals. Single crystals are primarily used in optical applications, and hence, an optical transmittance window and the transparency lower cut-off wavelength (200–400 nm) are very important for the realization of the SHG output in the range for using lasers. The optical width of the as-grown SMTC crystal was compared with those of NaCl and MnCl_2 complex inorganic crystals. The as-grown SMTC crystal has good transparency in the UV–vis and IR regions, which ensures that the crystals can be used as sensor materials from the UV–vis to the IR ranges and may be considered as a potential candidate for photonic and optoelectronic applications [13]. A graph was plotted to estimate the value of the direct band gap using Tauc's relation. The Tauc's plot was drawn between $(\alpha h\nu)^2$ and $h\nu$, as shown in Fig. 5. The band gap value is obtained by extrapolating the linear portion of the graph to the $h\nu$ axis at $(\alpha h\nu)^2 = 0$. The estimated band gap of the as-grown SMTC is 5.4 eV.

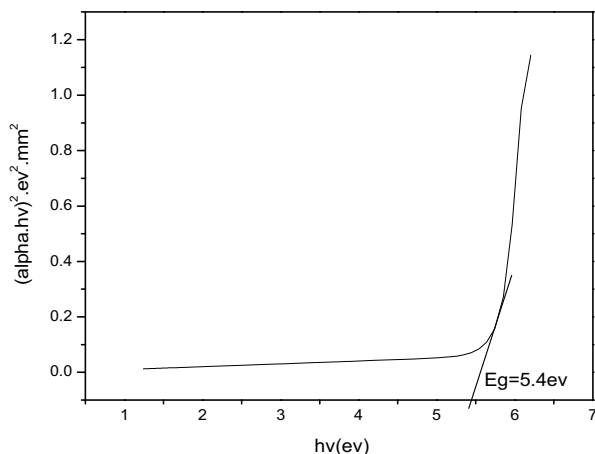


Fig. 5. Tauc's plot of SMTC crystal.

3.1.4. Second harmonic generation efficiency measurement

To confirm the nonlinear optical property, a powdered sample of SMTC was subjected to the Kurtz–Perry technique, which remains a powerful tool for the initial screening of materials for SHG [14]. The fundamental beam with a wavelength of 1064 nm from a Q-switched and mode-locked Nd:YAG laser was made to fall normally on the powder form of a ground sample, which was placed between two transparent glass slides. A pulse energy of 2.9 mJ/pulse and pulse width of 8 ns with a repetition rate of 10 Hz were used. A photomultiplier tube (Hamamatsu R2059) was used as a detector, and a 90 degree geometry was employed. The SHG signal generated in the sample was confirmed from the emission of bright green (532 nm) radiation from the sample. The measured amplitude of the second harmonic generation for the SMTC crystal is 11.32 mJ, and it is 8.8 mJ for KDP (a KDP crystal was powdered to the same size of the SMTC and used as a reference material). This result shows that the powder SHG efficiency of the SMTC crystal is approximately 1.3 times greater than that of KDP. The SHG efficiency of the SMTC crystal is compared to few popular inorganic NLO crystals, which are given in Table 1.

Table 1
comparison of SMTC crystal with other NLO crystals.

Compounds	SHG efficiency
Potassium dihydrogen phosphate (KDP)	1
Potassium pentaborate	0.79
Ammonium pentaborate	0.2
SMTC^a	1.32

^a Present work.

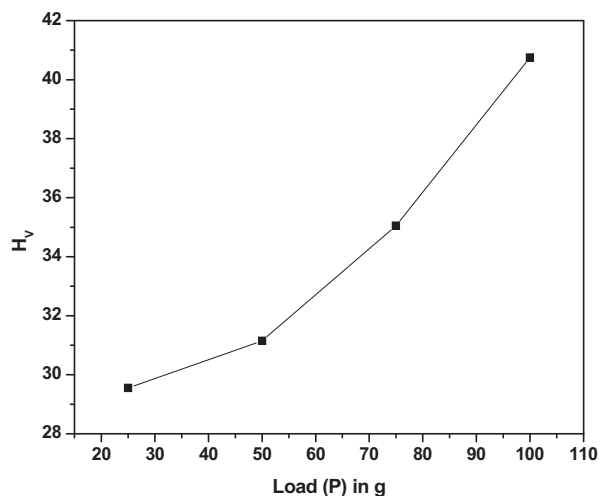


Fig. 6. Vickers hardness number against load plot of SMTC crystal.

3.1.5. Microhardness study

The mechanical property of the as-grown sample was investigated by measuring the hardness under various applied loads. A well-polished crystal was placed on the platform of the Vickers microhardness tester, and loads of different magnitudes were applied over a fixed duration of 5 s. Here, low loads are applied to measure the hardness of the samples. The microhardness analysis was performed using a Leitz Wetzlar hardness tester equipped with a diamond indenter. Indentations were made on the flat surface with the load ranging from 25 to 100 g using a Shimadzu HMV-2T equipped with a Vickers pyramidal indenter and attached to an incident light microscope. The indentation time was maintained at 5 seconds for all of the loads. Several indentations were made on the crystal surface with sufficient space for each load, and the diagonal length (d) of the indented impressions was measured. The Vickers hardness number of the materials, H_v , were determined by the relation $H_v = 1.8544P/d^2$ kg/mm², where P is the applied load in kg and d is the diagonal length of the indentation impression in mm. The hardness number was found to increase as the load increased, and above 100 g, significant cracks and inclusions were observed, which may be due to the release of internal stress generated locally by indentation [15]. The average value of the Vickers hardness number for the as-grown crystal is 100 kg/mm². A plot of the corresponding loads versus the hardness values of SMTC is shown in Fig. 6. The work-hardening coefficient (n) of the material is related to the load (p) by the relation $P = Ad^n$, where A is an arbitrary constant. The work-hardening coefficient ' n ' of the sample was determined from the slope of the plot of $\log p$ vs $\log d$ (Fig. 7), and it was found to be 2.278, indicating that the crystal

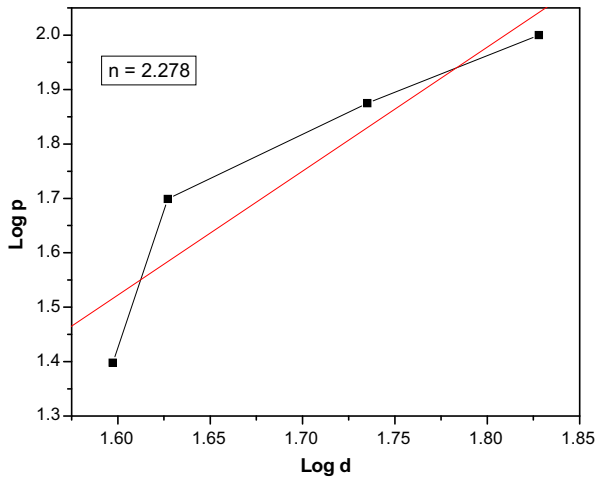


Fig. 7. Log *p* vs log *d* plot of SMTC crystal.

belongs to the soft category. From careful observations of various materials, Onitsch and Hanneman noted that a value of *n* between 1.0 and 1.6 indicates a moderately hard material and that a value of *n* greater than 1.6 represents a soft material [16,17]. The obtained value of *n* indicates that the SMTC crystal has a high mechanical strength and will be used in device applications.

3.1.6. Dielectric studies

The behaviour of the crystal under the influence of an electric field has a direct relation with the laser irradiation on the sample; hence, the power dissipation factor can be investigated from the dielectric studies. Dielectric studies of the SMTC single crystal were conducted as a function of frequency for various temperatures. Both sides of the SMTC crystal were coated with graphite to form an electrode for a parallel plate capacitor. The dielectric constant was calculated using the formula:

$$\epsilon_r = \frac{Ct}{\epsilon_0 A}$$

where *C* is the capacitance, *t* is the thickness of the crystal, ϵ_0 is the permittivity of the free space, and *A* is the area of a cross section of the sample. The variations in the dielectric constant and dielectric loss as a function of frequency (500 Hz–5 MHz) at different temperatures (308–368 K) are shown in Figs. 8 and 9. The inserted figures in Figs. 8 and 9 show that the variation of dielectric constant and dielectric load in the range of log frequency 4–7 at different temperatures. The dielectric constant is observed to be a function of frequency and temperature, which reveals that the dielectric constant decreases with increasing frequency. This behaviour of the sample is referred to as anomalous dielectric dispersion. A high

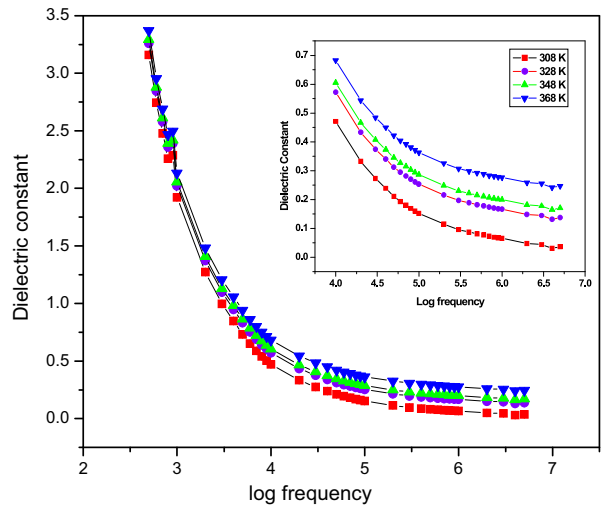


Fig. 8. Variation of dielectric constant of SMTC single crystal with log frequency at different temperatures.

dielectric constant at low frequency is attributed to various polarization mechanisms of molecules. In general, polarization occurs as a function of time. It is obvious that at lower frequencies, the time required for polarization is high. Hence, irrespective of the polarization mechanisms, the measurement of the dipole moment per unit volume would be high, resulting in the dielectric constant being independent of the frequency. At high frequency, a change in polarization occurs even at very short time. Therefore, polarization can occur only by the movement of electronic charges rather than the movement of ions, resulting in a low dielectric constant. Electronic and space charge polarization predominantly in the low-frequency region suggest that the as-grown

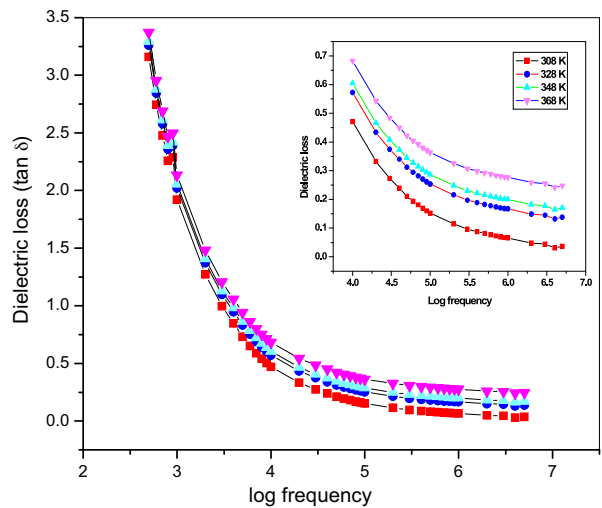


Fig. 9. Variation of dielectric loss of SMTC single crystal with log frequency at different temperatures.

crystal possesses an enhanced optical quality with fewer defects, and this phenomenon is an essential characteristic for nonlinear optical applications [18–20].

As shown in Fig. 9, the value of the dielectric loss is high in the low-frequency region, and the dielectric loss is too low at higher frequencies. The measured low dielectric loss at higher frequencies is due to the dipole rotation. Additionally, at high frequencies, the orientation polarization ceases and energy does not need to be spent to rotate dipoles. It is also observed that both the dielectric constant and dielectric loss depend on the temperature and increase slightly with increasing temperature at a constant frequency. It is believed that materials with a high dielectric constant lead to power dissipation. The refractive index of the medium is related to the dielectric constant according to the equation $n = (\epsilon_r \mu_r)^{1/2}$. For non-magnetic materials, μ_r is equal to one. This equation indicates that the electric field-based refractive index of the medium could play a vital role in nonlinear effects. SMTC crystals possess a low dielectric constant and low dielectric loss, and hence, these crystals will be suitable for electro-optic applications. Moreover, the low value of dielectric loss at high frequency can be considered as proof for the good optical quality of the crystal. The application of nonlinear optics requires high-quality crystals with minimal defects.

3.1.7. Photoconductivity studies

A photoconductivity study of the SMTC crystal was performed by connecting the sample in series with a DC power supply and a picoammeter (Keithley 480) at room temperature. The details of the experimental setup are reported elsewhere [21]. By increasing the applied field from 10 to 150 V/cm, the corresponding dark current without exposure to radiation was recorded. The photocurrent was recorded by exposing the crystal to a halogen lamp with a power of 100 W containing iodine vapour for the same applied field. The dark current and photocurrent against an applied field of the same range were recorded in the same graph (Fig. 10). From the graph, it is observed that the dark current and photocurrent of the as-grown crystal increased linearly with applied field, but the photocurrent increased less than the dark current. This phenomenon is referred to as negative photoconductivity.

The negative photoconductivity of the as-grown SMTC crystal may be due to a decrease in either the number of free charge carriers or their lifetime when subjected to radiation. The negative photoconductivity of the as-grown crystal can be explained according to the Stockman model, as follows: the forbidden gap in the material contains two energy levels, in which one

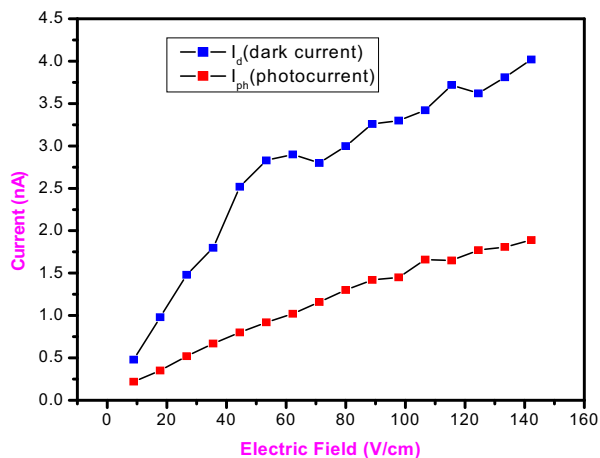


Fig. 10. Field dependent conductivity of SMTC crystal.

is situated between the Fermi level and the conduction band, while the other is located close to the valence band. The second state has a high capture cross section for electrons and holes. When it captures electrons from the valence band, the number of charge carriers in the conduction band decreases, and the current decreases in the presence of radiation [22,23].

3.1.8. Chemical etching analysis

Chemical etching analysis is one of the most convenient and suitable techniques for characterizing growth defects. High-quality crystals or crystals with well-defined defect structures are currently more important for device fabrication and technical applications. In general, crystals grown from solution may suffer from imperfections such as solvent inclusions, twins, grain boundaries and dislocations. When defect crystals are incident to a laser beam, the defects cause scattering and absorption of the laser beam. Hence, defects will affect the performance and use of crystals in laser applications. Generally, the etch patterns are captured at the dislocation sites by etching the crystal surface using suitable etchants [24]. The dissolution of a crystal in an etchant is an essential criterion for the formation of etch pits. The region where the dislocations intersect the surface of a crystal is energetically different from the surrounding area. In the present study, chemical etching was performed using ethanol at room temperature. After the damaged surface layer was removed by etching, a fresh surface appeared, which in turn provided clear etch pits. The etched surfaces were dried using good quality filter paper, and the surfaces were examined immediately. The etching study was conducted for different times, namely, 5 s, 10 s and 15 s, and the observed etch patterns are shown in Fig. 11a–c, respectively. In figure a,

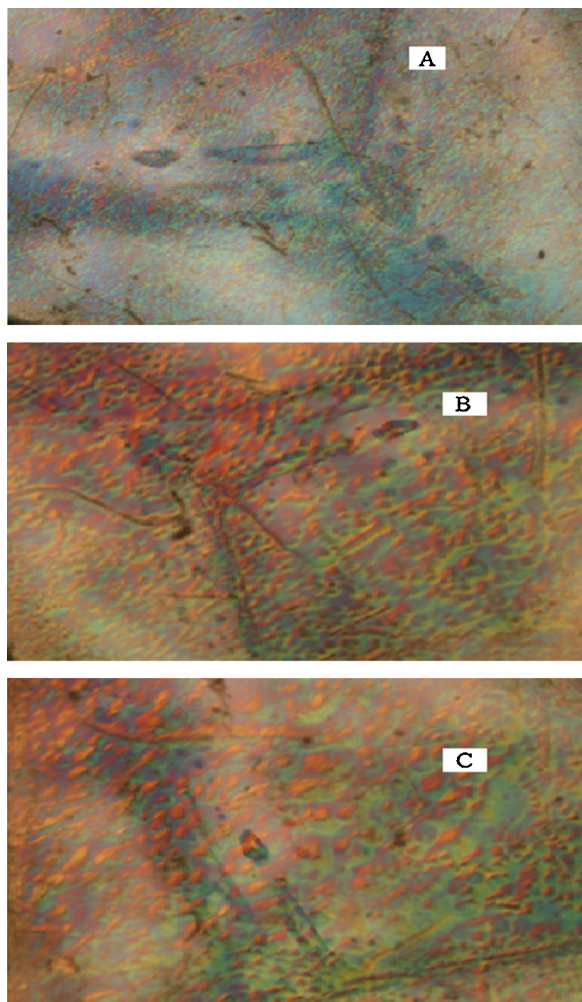


Fig. 11. Etch pattern on the SMTC crystal (A) after etching for 5 s, (B) after etching for 10 s, (C) after etching for 15 s.

whisker-type pits can be observed. Additionally, in an etched surface, shallow and deep etch pits are observed. By increasing the etching time, there is no change in the shapes, but the size of the pits slightly increased (Fig. 11b and c). The geometry of an etch pit also depends on the interatomic arrangement on the crystal. The observed etch pitch on the as-grown crystal surface implies that the crystal undergoes selective dissolution during growth.

4. Conclusion

A potential inorganic nonlinear optical single crystal of sodium manganese tetrachloride was prepared at room temperature through the slow evaporation of aqueous solutions. A well-defined external appearance with bright, transparent and colourless crystals were obtained. The unit cell parameters and the space group were

determined using single crystal data. The good crystalline nature of the SMTC was confirmed from the well-defined peaks in the powder X-ray diffraction patterns. The as-grown crystal shows 99% transmission with a UV cut-off at 240 nm; hence, it is suitable for frequency conversion applications. The SHG efficiency of the SMTC was measured to be higher than that of KDP. From the mechanical measurements, it was observed that the hardness increased with increasing load. The dielectric constant and dielectric loss studies of SMTC established the normal behaviour. The above experimental results, such as the bulk size, extremely good crystalline perfection, optical transparency, SHG efficiency and mechanical strength, may have possible implications for NLO applications.

References

- [1] A.H. Reshak, H. Kamarudin, S. Auluck, Acentric nonlinear optical 2,4-dihydroxyl hydrazone isomorphous crystals with large linear, nonlinear optical susceptibilities and hyperpolarizability, *J. Phys. Chem. B* 116 (2012) 4677–4683.
- [2] A.H. Reshak, I.V. Kityk, S. Auluck, Investigation of the linear and nonlinear optical susceptibilities of KTiOPO_4 single crystals: theory and experiment, *J. Phys. Chem. B* 114 (2010) 16705–16712.
- [3] F. Peter, M. Bordui, F. Martin, *Annu. Rev. Mater. Sci.* 23 (1993) 321–379.
- [4] P.N. Prasad, D.J. Williams, *Introduction to Nonlinear Optical Effects in Organic Molecules and Polymers*, John Wiley & Sons, Inc., New York, USA, 1991.
- [5] H.O. Marcy, L.F. Warren, M.S. Webb, C.A. Ebbers, S.P. Velsko, G.C. Kennedy, G.C. Catella, Second harmonic generation in zinc tris(thiourea) sulfate, *Appl. Opt.* 31 (1992) 5051–5060.
- [6] X.Q. Wang, D. Xu, D.R. Yuan, Y.P. Tian, W.T. Yu, S.Y. Sun, Z.H. Yang, Q. Fang, M.K. Lu, Y.X. Yan, F.Q. Meng, S.Y. Guo, G.H. Zhang, M.G. Jiang, Synthesis, structure and properties of a new nonlinear optical material: zinc cadmium tetrathiocyanate, *Mater. Res. Bull.* 34 (1999) 2003–2011.
- [7] P.A. Franken, A.E. Hill, C.W. Peters, G. Weinreich, Generation of optical harmonics, *Phys. Rev. Lett.* 7 (1961) 118–119.
- [8] H. Nalwa, S. Miyata, *Nonlinear Optics of Organic Molecules and Polymers*, CRC Press, New York, 1996.
- [9] C.F. Dewey Jr., W.R. Cook Jr., R.T. Hodgson, J.J. Wynne, Frequency doubling in $\text{KB}_5\text{O}_8 \cdot 4\text{H}_2\text{O}$ and $\text{NH}_4\text{B}_5\text{O}_8 \cdot 4\text{H}_2\text{O}$ to 217.3 nm, *Appl. Phys. Lett.* 26 (1975) 714–716.
- [10] D.S. Chemla, J. Zyss, *Nonlinear Optical Properties of Organic Molecules and Crystals*, Academic Press, Orlando, NY, 1987, pp. 01–02.
- [11] J. Goodyear, S.D.A. Ali, G.A. Steigmann, The crystal structure of Na_2MnCl_4 , *Acta Cryst. B* 27 (1971) 1672–1674.
- [12] R. Sankar, C.M. Raghavan, M. Balaji, R. Mohan Kumar, R. Jayavel, Synthesis and growth of triaquaglycinesulfatozinc(II), $[\text{Zn}(\text{SO}_4)(\text{C}_2\text{H}_5\text{NO}_2)(\text{H}_2\text{O})_3]$, a new semiorganic nonlinear optical crystal, *Cryst. Growth Des.* 7 (2007) 348–353.
- [13] Y. Le Fur, R. Masse, M.Z. Cherkaoui, J.F. Nicoud, *Z. Kristallogr.* 856 (1993).
- [14] S.K. Kurtz, New nonlinear optical materials, *IEEE J. Quantum Electron.* 4 (1968) 578–584.

- [15] T. Balakrishnan, K. Ramamurthi, Growth, structural, optical, thermal and mechanical properties of glycine zinc chloride single crystal, *Mater. Lett.* 62 (2008) 65–68.
- [16] E.M. Onitsch, The present status of testing the hardness of materials, *Mikroskopie* 95 (1956) 12–14.
- [17] M. Hanneman, *Metall. Manch.* 23 (1941) 135.
- [18] C. Balarew, R. Dublew, Application of the hard and soft acids and bases concept to explain ligand coordination in double salt structures, *J. Solid State Chem.* 55 (1984) 01–10.
- [19] P.V. Dhanaraj, N.P. Rajesh, Growth and characterization of non-linear optical γ -glycine single crystal from lithium acetate as a solvent, *Mater. Chem. Phys.* 115 (2009) 413–417.
- [20] K.V. Rao, A. Samakula, Dielectric properties of cobalt oxide, nickel oxide and their mixed crystals, *J. Appl. Phys.* 36 (1965) 2031–2038.
- [21] F.P. Xavier, A. Regis Indigo, G.J. Goldsmith, Role of metal phthalocyanine in redox complex conductivity of polyaniline and aniline black, *J. Porphyr. Phthalocyanines* 3 (1999) 679–686.
- [22] V.N. Joshi, *Photoconductivity*, Marcel Dekker, New York, 1990.
- [23] S. Abraham Rajasekar, K. Thamizhrasan, J.G.M. Jesudurai, D. Premanand, P. Sagayaraj, The role of metallic dopants on the optical and photoconductivity properties of pure and doped potassium pentaborate (KB5) single crystal, *Mater. Chem. Phys.* 84 (1) (2004) 157–161.
- [24] K. Owczarek, Sangwal, Effect of impurities on the growth of KDP crystals: On the mechanism of adsorption on {1 0 0} faces from tapering data, *J. Cryst. Growth* 99 (1990) 827–831.